HHS Public Access

Author manuscript

Lancet Respir Med. Author manuscript; available in PMC 2021 June 01.

Published in final edited form as:

Lancet Respir Med. 2020 June ; 8(6): 573–584. doi:10.1016/S2213-2600(19)30356-X.

Small airways pathology in Idiopathic Pulmonary Fibrosis: A retrospective cohort study

Stijn E. Verleden, Ph.D.[*], **Naoya Tanabe, M.D.**[*], **John E. McDonough, Ph.D.**, **Dragoş M. Vasilescu, Ph.D.**, **Feng Xu, Ph.D.**, **Wim A. Wuyts, M.D.**, **Davide Piloni, M.D.**, **Laurens De Sadeleer, M.D.**, **Stijn Willems, Ph.D.**, **Cindy Mai, M.D.**, **Jeroen Hostens, Ph.D.**, **Joel D. Cooper, M.D.**, **Erik K. Verbeken, M.D.**, **Johny Verschakelen, M.D.**, **Craig J. Galban, Ph.D.**, **Dirk E. Van Raemdonck, M.D.**, **Thomas V. Colby, M.D.**, **Marc Decramer, M.D.**, **Geert M. Verleden, M.D.**, **Naftali Kaminski, M.D.**, **Tillie-Louise Hackett, Ph.D.**, **Bart M. Vanaudenaerde, Ph.D.**[*], **James C. Hogg, M.D.**[*]

Department of Clinical and Experimental Medicine, Division of Respiratory diseases, (S.E.V., J.E.M., Prof. W.A.W., D.P., L.D.S., S.W., Prof. E.K.V., Prof. D.E.V.R., Prof. M.D., Prof. G.M.V., B.M.V.); Department of Radiology, (C.M., Prof. J.V.) - all KU Leuven - University of Leuven, University Hospitals Leuven, B-3000 Leuven, Belgium; the University of British Columbia, Department of Pathology and Center for Heart and Lung Innovation, located at St. Paul's Hospital, Vancouver, British Columbia, Canada (N.T., D.M.V., F.X., T-L.H., Prof. J.C.H.); Department of Respiratory Medicine, Graduate School of Medicine, Kyoto University, Kyoto, Japan (N.T.); the Respiratory Disease Unit, Fondazione IRCCS Policlinico San Matteo, University of Pavia, Pavia, Italy (D.P.); the Bruker microCT, Kontich, Belgium (J.H.); the Department of Thoracic Surgery University of Pennsylvania, Philadelphia, PA, USA (Prof. J.D.C.); the Department of Radiology, University of Michigan, Ann Arbor, Michigan (C.J.G.); the Section of Pulmonary, Critical care and Sleep Medicine, Yale University, New Haven, Connecticut (Prof. N.K.); the Department of Laboratory Medicine and Pathology, Mayo Clinic Arizona (Prof. T.V.C.).

Abstract

Background: The observation that patients with Idiopathic Pulmonary Fibrosis (IPF) can achieve higher than normal expiratory flow rates at the low lung volumes where they are forced to breathe, led naturally to the conclusion that the airways are spared in IPF. This study re-examines the hypothesis that airways are spared in IPF using a multi-resolution imaging protocol that combines multi-detector computed tomography (MDCT), with microCT and histology.

Reprint requests to Dr. James C. Hogg at the University of British Columbia, Centre for Heart Lung Innovation, St. Paul's Hospital, Rm166, 1081 Burrard Street, Vancouver, B.C., V6Z 1Y6, Canada or at Jim.Hogg@hli.ubc.ca.

[*] contributed equally to this work.

CONTRIBUTORS

S.E.V*., N.T*., J.E.M., D.M.V., F.X., W.A.W., D.P., L.D.S., S.W., C.M., J.V., C.J.G., T.V.C., and T-L.H. contributed to data collection, analysis and interpretation. J.H., J.C., E.K.V., D.E.V.R., M.D., G.M.V., B.M.V., and J.C.H., contributed to the conception, hypothesis delineation, and design of the study. S.E.V., N.T., D.M.V., M.D., G.M.V., N.K., T-L.H., B.M.V*., and J.C.H*., *contributed to writing the manuscript.

DECLARATION OF INTERESTS

All other authors declare no competing interests.

Methods: A cohort of explanted lungs from patients with severe IPF treated by lung transplantation (n=11), were compared to a cohort of unused donor (control) lungs (n=10), that provided 240 samples of lung tissue for comparison using the multi-resolution imaging approach.

Findings: The MDCT specimen scans show that airways located between the 9th and 14th generations of airway branching increase their visibility in IPF due to thickening of their walls and distortion of their lumens. Further, the microCT analysis showed that compared to normal (control) lung anatomy, minimal fibrosis in IPF tissue is associated with a 60% reduction in terminal bronchioles, the appearance of fibroblastic foci and infiltration of the tissue by inflammatory immune cells capable of forming lymphoid follicles. Whereas, established fibrosis in IPF tissue is dominated by increased airspace size, Ashcroft fibrosis score, and volume fractions of tissue and collagen.

Interpretation: Small airways disease is a feature of IPF, with significant loss of terminal bronchioles occuring within regions of minimal fibrosis. Based on these findings, we postulate that the small airways could become a potential therapeutic target in IPF.

Funding: The study was funded by KULeuven (C24/15/30), the US National Institutes of Health research grant RO1HL127349 and R44HL118837, the BC lung association and Genentech.

Keywords

IPF; imaging; x-ray computed tomography (CT); microCT; histology

INTRODUCTION

The most recent American Thoracic Society and European Respiratory Society statement[1] on idiopathic pulmonary fibrosis (IPF) practice guidelines and novel therapeutics[2,3], credits Liebow and Carrington[4] for introducing the term Usual Interstitial Pneumonia (UIP) to describe the histopathology of IPF. Further, it credits Katzenstein[5], Nicholson[6], and their colleagues, for extending these observations to include the formation of small distinct fibroblastic foci that have become a well-recognized diagnostic feature of the histopathology of IPF. Since then, Cool et al.[7], have proposed that these fibroblastic foci are organized into a distinct network at the leading edge of a wave of fibrosis in IPF. However, this interpretation was recently challenged by Jones et al.[8], who used three dimensional (3D) micro-computed tomography (microCT) imaging combined with histology, to demonstrate that fibroblastic foci form a constellation of heterogeneous structures that vary considerably in shape and volume without any evidence of connectivity between them.

The concept that IPF is an interstitial lung disease that obliterates the alveoli but spares the airways is widely accepted in the literature. This hypothesis is supported by physiological observations that show patients with IPF can achieve much higher than normal expiratory flow rates at the low lung volumes where these patients are forced to breathe[9]. Fulmer et al. [10], were the first to link pathology in the small airways to abnormal lung physiology in patients with IPF more than 40 years ago, based on a qualitative assessment of small conducting airway pathology observed in the open lung biopsies obtained to make the diagnosis of IPF. Most recently, an extensive review of the genetics of IPF by Evans et al.[11], has defined IPF as a complex genetic disorder of mucociliary function that produces

peripheral airways pathology, based on the observation that the MUC5B promoter variant rs35705950, is the strongest and most frequently validated risk factor for IPF.

This report re-examines the hypothesis that the airways are spared in IPF using volumetric imaging which enables a quantitative assessment of the airway tree. A retrospective cohort study was performed on explanted lungs from IPF patients undergoing lung transplant, and unused donor control lungs, using a cascade of clinical multi-detector CT (MDCT), microCT, and histological imaging, originally developed to investigate small airways disease in COPD[12–14], and subsequent studies in lung allograft rejection[15] and cystic fibrosis[16].

METHODS

Subjects

Whole lungs were obtained from a cohort of end-stage IPF patients (n=11) undergoing lung transplantation, and a cohort of donor (controls, n=10) that had no known lung disease, comorbidities, or structural lung injury. All donor lungs were deemed appropriate for transplant on review of the clinical files, but were not used either due to no adequate recipient, the recipient dying before implantation, persistent embolism during procurement or in one case the identification of a kidney tumor. The control and IPF groups were matched for age, sex, height and weight. The diagnosis of IPF was established by a multidisciplinary consensus committee according to existing guidelines[1], and confirmed by video-assisted thoracic surgical biopsy in seven of the IPF patients, and by pathological examination of the contralateral lung in all ten patients affected by IPF. Informed consent was obtained directly from each IPF patient awaiting lung transplantation. Whereas permission to study the unused donor lungs that served as controls (n=11), was obtained either in accordance with Belgian law, where all eligible subjects automatically become donors and where organs of insufficient quality can be released for research or from the donors next of Kin under conditions that are described in detail by the gift of Life Donor Program (http://www.donors1.org). All of the procedures used in these studies were approved by both the ethics (S52174) and biosafety (MS20101571) committees at KU Leuven and agreed to through material transfer agreements between KU Leuven by all the other institutions involved. The demographic and clinical characteristics of all donors are presented in Table 1.

Pre-operative CT analysis

Pre-operative inspiratory thoracic CT scans taken as part of routine standard of care, at the closest time point of transplant (median 33 days) were used for the analysis. MDCT scans for all IPF subjects were acquired using the following parameters (120–140kV, 80–140mA, 1–5mm slice thickness) by coaching the subject to inhale as deeply as possible in the supine position. The CT scans were scored by two experienced chest radiologist's (JV, CM) using the Fleischner Society guidelines[17] in all five lung lobes using a score from 0–3, the resulting score (max of 15), was then re-calculated to 100% to obtain the percentages of airway dilation, consolidation, ground glass opacities, air trapping, reticular pattern, volume loss, cyst formation and emphysema (Table 1).

Lung tissue processing

These procedures have been described in detail elsewhere.[13–15,18] Briefly, a single explanted lung from each subject was inflated with air to a transpulmonary pressure of 30cm H_2O, then deflated to 10cm H_2O and held constant while the lung was frozen in liquid nitrogen vapour. The frozen lung specimen was then imaged *ex vivo* by MDCT (120kV, 110mA, 1mm slice thickness) to calculate lung volume, density and mass. The frozen lung was then sliced into contiguous 2cm thick slices in the trans-axial plane, and slices were photographed before and after lung tissue samples 1·4 cm in diameter were extracted. Each lung and sample was given a unique 4 digit number to blind the analysis. Two sampling methods were used in this study:

Experiment 1: The samples used for microCT and histology were chosen at random by first numbering all the available sites on the lung slice photographs, then using a random number generator to select one sample from each slice (7–10 samples per lung). Samples were fixed overnight in 1% solution of glutaraldehyde in acetone that remains liquid at −80°C, warmed to room temperature, and chemically dehydrated in a graded series of ethanol concentrations followed by hexamethyldisilazane (Sigma-Aldrich, Belgium) treatment to complete the drying process. These fixed, dried samples were then imaged using a Skyscan 1172 microCT scanner (Bruker, Belgium) at 8·4 μm voxel resolution.

Experiment 2: Samples were selected from regions of minimal and established fibrosis identified by the radiologists in the upper, middle and lower regions of each lung using the MDCT scans of the frozen specimens (6 samples per lung). The lung samples were kept frozen (−30°C) using a cryostage (Bruker, Belgium) while they were examined by microCT at 9·9 μm resolution. These samples were then vacuum embedded in cryomatrix for subsequent examination by histology. Seven of the patients with IPF and three of the control subjects were included in both experiment 1 and 2 (see footnote - table 1).

Micro-CT analysis

Terminal bronchioles were identified anatomically and counted per millilitre of lung tissue as previously described.[12] The total number of terminal bronchioles/lung was computed as the product of the mean number/ ml lung in all sampled cores of tissue and total lung volume measured from the *ex vivo* MDCT scan, using custom-made software. Ten systematic uniform randomly sampled image slices from the microCT scans of each tissue core were extracted and used to measure the mean linear intercept (Lm) using a line-grid[12] in Image-Pro Plus (Version 5.1, Media Cybernetics, Silver Spring, USA). The method described by Tanabe et al.[14], was used to measure pre-terminal bronchiole wall area, number of alveolar attachments, luminal area and circularity. We have previously demonstrated that lung tissue samples scanned following glutaraldehyde fixation or frozen are comparable when assessed for Lm.[19]

Histological analysis

All histological analysis was performed on exactly the same samples examined by microCT from Experiment 2. The methods used to evaluate the histology in this report have been previously described in detail.[13] The extent of fibrosis present in the tissue was assessed

using the Ashcroft fibrosis score[20] and by calculating the volume fractions (Vv) of lung taken up by tissue, fibroblastic foci, and Vv of small airways and parenchymal tissue staining positive for collagen using the picrosirius red stain. The Vv of the tissue containing tertiary lymphoid organs and the Vv of small airways and parenchymal tissue staining positive for individual inflammatory cells; neutrophils (NP57), macrophages (CD68), B-cell (CD79a), eosinophils (major basic protein), CD4 and CD8 lymphocytes were also assessed. A list of antibodies is provided in Table S1 in the online supplement.

Statistical analysis

The Mann-Whitney test was used to compare the patient demographics, terminal bronchiolar counts, terminal bronchiolar dimensions and parenchymal dimensions between IPF and control. A Kruskall Wallis with Dunn's post hoc test was used to compare terminal bronchiolar dimensions, and immunohistochemistry data between minimal and established fibrosis, and controls. Bland-Altman plots were used to compare inter-observer comparisons. Analysis were performed by sample, except for values that are presented by case (total number of terminal bronchioles, lung volume, lung mass, lung density). The number of airways per generation was compared using two-way ANOVA with Tukey's post hoc test. The statistical analysis was performed using the R statistical program (version 3.2.1) or Graph pad prism 6.0 (Graph pad, La Jolla, CA, USA). The sample size was based on the available donor lungs and our experience in previous studies[12,15,21]. Data are expressed as the mean ± SD. A p value <0·05 was considered significant.

Role of Funding Source

The study was funded by KULeuven (C24/15/30), the US National Institutes of Health research grant RO1HL127349 and R44HL118837, the BC lung association and Genentech. The study sponsors had no role in the design, collection, and analysis, interpretation of the data, writing or submission of the manuscript. The corresponding author had full access to all of the data and the final responsibility to submit for publication.

RESULTS

Patient Characteristics

Experiment 1 included eight control and nine IPF lung specimens, and experiment 2 included six control and nine IPF lung specimens, three of the control and seven of the IPF lungs were included in both of the experiments. There was no difference in the sex, age, height, and weight between the control and IPF subjects. The majority of the controls were non-smokers, while all but one of the IPF subjects were ex-smokers (Table 1). The lung function data and preoperative MDCT scans were not available for the control subjects. There were no differences in lung function and MDCT radiological scoring between IPF subjects in experiment 1 (randomly sampled) and experiment 2 (targeted sampling for minimal and established fibrosis).

Quantification of airways in IPF by MDCT

Analysis of the *ex vivo* MDCT lung specimen scans shows patients affected with severe IPF have a significant reduction in total lung volume, and an increase in total lung tissue volume,

mass and density (Table 2). In addition, using the 800μM spatial resolution provided by the *ex vivo* MDCT specimen scans, the concentration of visible airways increased from 125±36 airways/litre of lung in the controls to 572±222 airways/litre of lung in IPF subjects (p<0·0001, Table 2). Further, the total number of visible airways/lung increased from 402±114 airways/lung in the controls to 811±251 airways/lung in IPF subjects (p=0·0055, Table 2). Figure S1 in the online supplement shows that the inter-observer variability for counting airways on MDCT was small. In Figure 1A, these data are visualized by airway generation and show that the number of airways in IPF lungs increased between the 9th and 14th generations of airway branching compared to control lungs, and primarily involved airways <2mm in diameter (Figure 1B). Further, Figure 1 also shows that compared to normal (control) lung anatomy (Figure 1C, D, E) regions of minimal fibrosis in IPF tissue (Figure 1F, G, H), is associated with the collapse of alveoli onto the alveolar ducts. Whereas established fibrosis (Figure1 I, J, K) is associated with the infiltration of both the alveolar wall and peribronchovascular interstitial spaces by fibrous connective tissue mixed with extra-vascular fluid in both the alveolar wall and peribronchovascular interstitial spaces.

Quantification of small airways in IPF by microCT

Using the 8·4 and 10 μm voxel resolution of the microCT scans it is possible to quantify the morphometry of small airways <2mm in diameter (terminal and pre-terminal bronchioles). As shown by the representative cross-sectional images from a control (Figure 2A) and IPF pre-terminal bronchiole within a sample with minimal (Figure 2B) and established fibrosis (Figure 2C), pre-terminal bronchioles from IPF patients had a significant increase in wall area (p<0·0001, Figure 2D), and decreased lumen circularity (p<0·0001, Figure 2E) irrespective of whether the sample was from a region of minimal or established fibrosis. Whereas alveolar attachments tethering the pre-terminal bronchiole wall were decreased in regions of established fibrosis (p=0·0142, Figure 2F). As shown in Figure 2G, there was no difference in luminal area between the groups.

The minimal diameter (p=0·0480) and minimal area (p=0·0480) of terminal bronchioles was significantly increased in IPF subjects compared to controls (Table 2). The Bland-Altman plots (Figure S2 in the online supplement) show good agreement between the two independent observers for counting the number of terminal bronchioles in controls and IPF. In addition, lungs from patients with IPF showed a significant reduction in the number of terminal bronchioles/ml compared to controls (Figure 3A, p<0·0001). Further, the number of terminal bronchioles was reduced in IPF lungs in areas of both minimal and established fibrosis. When assessed for airspace size, only regions of established fibrosis had a significant increase in Lm compared to minimal fibrosis (Figure 3B, p<0·0001). In a sub analysis by smoking history, the number of terminal bronchioles/ml was significantly reduced in IPF patients with <5 years or >20 years pack year history compared to control smokers irrespective of the number of pack years. Further, the reduction in the number of terminal bronchioles was the same in IPF smokers with a high or low pack year history (Figure S3 in the online supplement).

Quantification of IPF lung tissue by histology

Histological analysis of Lm confirmed the finding by microCT that airspace size is increased within regions of established fibrosis compared to minimal fibrosis in IPF lungs, and control lung samples (p=0·0323 and p<0·0001, Figure 4A). Further, the Ashcroft fibrosis score on histology was greater in samples of established compared to minimal fibrosis (p<0·0001, Figure 4B). Compared to controls and minimal fibrosis in IPF tissue, lesions of established fibrosis in IPF samples were associated with a progressive increase in the Vv of lung taken up by tissue (p<0·0001, Figure 4C), and the Vv of collagen identified by picro sirius red staining in the parenchyma (p=0·0056, Figure 4C), but not in the small airways (Figure 4D). Similar numbers of fibroblastic foci were present in IPF samples from regions of minimal and established fibrosis (Figure 4E).

As shown in Figure 5A compared to controls, minimal and established fibrosis in IPF is associated with an increase in the Vv of B-cells (p=0·0037 and p=0·0007) and CD4 (p=0·0022 and p=0·0074) lymphocytes in the small airways, and an increase in the Vv of macrophages (p<0·0001 and p=0·0038), B-cells (p<0·0001 and p<0·0001), CD4 (p<0·0001 and p<0·0001), CD8 (p<0·0001 and p<0·0001) lymphocytes in the parenchyma. The infiltration of these cells within the tissue is also associated with an increase in the Vv of non-encapsulated tertiary lymphoid organs (Figure 5B), in both regions of minimal and established fibrosis (P=0.0068 and p=0·0011, Figure 5C).

DISCUSSION

To our knowledge this report provides the first direct evidence that in IPF lungs the small airways <2mm in diameter on thoracic MDCT scans increase their visibility due to thickening of their airway walls and distortion of their airway lumens. Further, compared to normal (control) lung anatomy, regions of minimal fibrosis in IPF lungs assessed by high resolution microCT are associated with a 60% reduction in the number of terminal bronchioles, as well as the appearance of fibroblastic foci and non-encapsulated lymphoid follicles. Importantly, regions of established fibrosis in IPF did not show a further decline in the number of terminal bronchioles, but were associated with an increase in airspace size, Ashcroft fibrosis score, and volume fraction of tissue and collagen; consistent with progressive fibrosis. These data indicate that the pathology in the small airways is an early feature of IPF.

Hamman and Rich commented on the presence of small conducting airways disease in their classic 1944 description of the pathology of rapidly progressive IPF.[22] However, physiological observations made in the 1950's and 60's, showing that patients affected by IPF can achieve much greater than normal airflows at the low lung volumes where they are forced to breathe[9], led naturally to the hypothesis that IPF is a disease that destroys the alveoli, but spares the airways. Thus, many subsequent investigations on the pathology of IPF focused on the changes that occur within the alveolar and bronchovascular interstitium.[23] In the current study, we used multi-resolution volumetric imaging, random sampling, and immunohistochemistry to assess small airways disease in IPF.

The analysis of the *ex vivo* (explanted) lung specimens using MDCT, demonstrate that IPF is associated with an increased visibility of smaller airways approximately 2mm in diameter located between the 9th and 14th generations of airway branching. Using the ultra-resolution of microCT in lung tissue samples we were able to demonstrate that small airways had thickened walls and distorted lumens. We therefore propose that the reason there are more visible small airways on MDCT is that airway wall thickening and distortion of the lumen brings these airways into the visible range at the spatial resolution provided by MDCT, rather than the alternative hypothesis that IPF patients are either born with more airways or develop more airways with disease. However, this needs to be investigated in more detail using MDCT to assess a longitudinal population based cohort. This study, also confirmed an earlier report by Coxson et al.[24] showing that an MDCT scan can be used to quantify a reduction in total lung volume, an increase in tissue volume, density and mass of IPF lungs, compared to control donor lungs.

The microCT results demonstrate that compared to normal (control) lung anatomy, regions of minimal fibrosis diagnosed by the radiologists on the preoperative thoracic MDCT scans of IPF patient's show a 60% reduction in the numbers of terminal bronchioles/ml of lung. When the microCT analysis was coupled with histology we found loss of terminal bronchioles was associated with the appearance of fibroblastic foci as well as an increase in the volume fraction of fibroblastic foci. Further, minimal fibrosis in IPF lungs was also associated with the appearance and increase in volume fraction of infiltrating inflammatory immune cells dominated by lymphocytes, and with an increase in the volume fraction of non-encapsulated lymphoid follicles. Follicular bronchiectasis was first coined by Whitwell.[25] It was later understood that the formation of germinal centres within these lymphoid follicles establishes the presence of an adaptive immune response.[26] In COPD, lymphoid follicles associated with small airways have been shown to increase in number with disease severity.[27] Such a host immune response is now recognized as a field immune response[28], capable of mounting both an innate and adaptive host immune response to protect the mucosal surfaces of the gastrointestinal, respiratory, genitourinary tracts as well as the skin.

In interstitial lung disease, lymphoid follicles are generally considered a hallmark of connective tissue disease. Following review of all of the IPF cases in this study by an experienced multidisciplinary board of experts[29] including a rheumatologist following the current guidelines[1]. We found that one patient in experiment 1, and one patient in experiment 2 had a positive test for antinuclear factor, however no other indications for systemic disease could be found. Further, nine years post-transplant, these patients still have had no other evidence for an auto-immune disease. As these patients did not show any other symptoms by clinical and morphologic phenotyping, a diagnosis of interstitial pneumonia with autoimmune features (IPAF) could not be made[30]. Further, we found no difference in the airway counts, number of terminal bronchioles or histological staining between these two patients compared to all other IPF patients in the study. We therefore believe the lymphoid follicles observed in all IPF patients in this study are not likely due to autoimmune disease, but rather they demonstrate an adaptive immune response within the tissue.

In comparison to minimal fibrosis, regions of established fibrosis were dominated by the infiltration of the alveolar and peribronchovascular interstitial spaces by fibrous connective

tissue that creates a modest increase in airspace size by dilating and distorting the alveolar ducts to form micro cysts that are clearly visible by microCT, but considerably smaller than the honeycomb cysts and traction bronchiectasis that are a well-established features of the pathology of IPF.[17] Further, the progressive increase in fibrosis from minimal to established fibrosis was associated by an increase in the Ashcroft fibrosis score and volume fractions of the lung occupied by tissue and collagen, without any change in either the volume fraction of fibroblastic foci or lymphoid follicles.

Based on these findings, the hypothesis that the airways are spared in IPF is rejected in favour of an alternative put forward by Mead in 1970[31] who postulated that the small conducting airways <2mm in diameter represent a “quiet zone” within the lungs where disease can accumulate over many years without being noticed by either the patient with the disease or the clinicians responsibible for their care. Indeed, Mead’s hypothesis has now been supported in a study of COPD by Koo et al.[32], that used the same combination of MDCT, microCT and histology to demonstrate that 41% of terminal bronchioles are already lost in the lungs of patients with mild (GOLD1) COPD. In addition, studies by Kawabata et al.[33] and Katzenstein and colleagues[34], have also reported histological evidence of fibrosis including fibroblastic foci, focal honey-combing, peribronchiolar metaplasia and respiratory bronchiolitis as common findings in lobectomy specimens from patients being treated for lung cancer where there was no clinical evidence of interstitial lung disease. Further, CT based studies have identified interstitial lung abnormality even in subjects without a prior history of interstitial lung disease, and that this radiological finding is associated with impaired pulmonary function and poor prognosis.[35] These studies provide initial evidence which is consistent with the hypothesis that IPF has a preclinical phase identified only histologically. Such work also deserves further investigation with respect to a series of studies that have established that IPF and emphysema are commonly observed in lungs from the same patient.[36] To this end it will be important to determine if new *in vivo* imaging methodologies such as parametric response mapping[37] which have now been validated by microCT[38] to identify functional small airways disease (terminal bronchiole thickening and narrowing) in COPD can be used to identify early disease alterations in IPF.

Although the results reported here highlight small airways disease in IPF they must be considered preliminary based on the relative small number of IPF lungs examined. Firstly, while this retrospective cohort study was matched for sex, age, height, and weight to reduce confounding variables all but one IPF patient in this study were former smokers, which means that the data may not be generalizable to all IPF patients, particularly patients with no smoking history. However, our sub-analysis of the data by smoking history found that terminal bronchiole numbers were reduced to the same extent in IPF patients compared to controls with and without smoking history whether IPF patients had <5 or >20 pack years smoking history.

Secondly, the fact that all of the lungs came from IPF patients with end-stage disease, where treatment by lung transplantation was the only option, it does not allow one to observe the progression of the disease over time, or determine if the patients with IPF may have been born with a smaller number of airways. Despite this, the use of transplant organs rather than biopsy tissue, allows for inflation of the tissue and assessment of disease within the whole

lung. Further, as most IPF patients die from generalized pulmonary infections it makes the assessment of post-mortem IPF lungs very difficult. Lastly, the pre-operative inspiratory thoracic CT scans used in the analysis were taken at the closest time point to transplant (median 33 days) as part of the patients' routine standard of care to rule out emboli and / or diagnose disease progression. At the time of these scans 4/9 patients in experiment 1 and 5/9 patients in experiment 2 were exacerbating which resulted in a relatively high percentage of ground glass opacities ((GGO), 46±27 and 57±9%, respectively). However, we do not believe GGO would have affected the airway counts conducted using MDCT, and certainly not the airway counts conducted using microCT on the excised lungs taken at the time of transplant when none of the patients were exacerbating.

In conclusion, these findings support the concept that pathology in the small conducting airways is a feature of IPF, with a significant loss of terminal bronchioles occurring within regions of minimal fibrosis. While further work is required to understand the role of the small conducting airways in IPF, we postulate that the findings reported here will stimulate discussion of how therapeutic interventions might target small airways disease to modify disease outcomes in IPF.

Supplementary Material

Refer to Web version on PubMed Central for supplementary material.

ACKNOWLEDGEMENTS

WW is a Senior Clinical Investigator of the Research Foundation Flanders and holds the Roche Crystal Chair in Interstitial Lung Diseases. SW is a doctoral research fellow of the Agency for Innovation by Science and Technology in Flanders. SEV is senior research fellow of FWO (12G8715N, 1503620N and G3C0494). JEM is funded by European Respiratory Society Respire2–2015-9192. NT is funded by the Dr. K. K. Pump Fellowship of the BC Lung Association. DMV is supported by Canadian Thoracic Society and Alpha-1 Foundation fellowships. TLH is supported by Canadian Institutes of Health Research, Michael Smith Foundation for Health Research Foundation, Parker B. Francis Foundation and Providence Health Care Research Institute new investigator awards. NK is funded by National Institutes of Health NHLBI grants R01HL127349, U01 HL145567, U01HL122626, U54HG008540, and R01HL141852. The authors would like to thank the James Hogg Lung Registry (Darren Sutherland), and Histology Core (Amrit Samra) from the Centre for Heart Lung Innovation, St. Paul's Hospital, Vancouver, Canada.

Dr. Tanabe reports grants from FUJIFILM, personal fees from Nippon Boehringer Ingelheim Co., Ltd., outside the submitted work. Dr. Wuyts reports grants from Roche, grants from Boehringer Ingelheim, outside the submitted work and all payed to the University. Dr. Decramer reports grants from Boehringer-Ingelheim, outside the submitted work. Dr. Kaminski reports personal fees from Biogen Idec, Boehringer Ingelheim, Third Rock, Miragen, Pliant, personal fees from Samumed, NuMedii, Indaloo, Theravance, LifeMax, Three Lake Partners, outside the submitted work; In addition, Dr. Kaminski has a patent New Therapies in Pulmonary Fibrosis with royalties paid to Biotech, and a patent Peripheral Blood Gene Expression issued and Serves as Deputy Editor of Thorax, BMJ.

REFERENCES

1. Raghu G, Remy-Jardin M, Myers JL, et al. Diagnosis of Idiopathic Pulmonary Fibrosis. An Official ATS/ERS/JRS/ALAT Clinical Practice Guideline. American journal of respiratory and critical care medicine 2018; 198(5): e44–e68. [PubMed: 30168753]
2. Noble PW, Albera C, Bradford WZ, et al. Pirfenidone in patients with idiopathic pulmonary fibrosis (CAPACITY): two randomised trials. Lancet 2011; 377(9779): 1760–9. [PubMed: 21571362]
3. Richeldi L, du Bois RM, Raghu G, et al. Efficacy and safety of nintedanib in idiopathic pulmonary fibrosis. N Engl J Med 2014; 370(22): 2071–82. [PubMed: 24836310]

4. Liebow AA CC. The interstitial pneumonias, frontiers of pulmonary radiology. New York: Grune and Stratton; 1969.

5. Katzenstein AL, Mukhopadhyay S, Myers JL. Erratum to “Diagnosis of usual interstitial pneumonia and distinction from other fibrosing interstitial lung diseases” [Hum Pathol 39 (2008) 1275–1294]. Hum Pathol 2008; 39(11): 1562–81. [PubMed: 19653362]

6. Nicholson AG, Fulford LG, Colby TV, du Bois RM, Hansell DM, Wells AU. The relationship between individual histologic features and disease progression in idiopathic pulmonary fibrosis. American journal of respiratory and critical care medicine 2002; 166(2): 173–7. [PubMed: 12119229]

7. Cool CD, Groshong SD, Rai PR, Henson PM, Stewart JS, Brown KK. Fibroblast foci are not discrete sites of lung injury or repair: the fibroblast reticulum. American journal of respiratory and critical care medicine 2006; 174(6): 654–8. [PubMed: 16799077]

8. Jones MG, Fabre A, Schneider P, et al. Three-dimensional characterization of fibroblast foci in idiopathic pulmonary fibrosis. JCI Insight 2016; 1(5).

9. Gibson GJ, Pride NB. Pulmonary mechanics in fibrosing alveolitis: the effects of lung shrinkage. Am Rev Respir Dis 1977; 116(4): 637–47. [PubMed: 921050]

10. Fulmer JD, Roberts WC, von Gal ER, Crystal RG. Small airways in idiopathic pulmonary fibrosis. Comparison of morphologic and physiologic observations. J Clin Invest 1977; 60(3): 595–610. [PubMed: 893665]

11. Evans CM, Fingerlin TE, Schwarz MI, et al. Idiopathic Pulmonary Fibrosis: A Genetic Disease That Involves Mucociliary Dysfunction of the Peripheral Airways. Physiol Rev 2016; 96(4): 1567–91. [PubMed: 27630174]

12. McDonough JE, Yuan R, Suzuki M, et al. Small-airway obstruction and emphysema in chronic obstructive pulmonary disease. N Engl J Med 2011; 365(17): 1567–75. [PubMed: 22029978]

13. Tanabe N, Vasilescu DM, Kirby M, et al. Analysis of airway pathology in COPD using a combination of computed tomography, micro-computed tomography and histology. Eur Respir J 2018; 51(2).

14. Tanabe N, Vasilescu DM, McDonough JE, et al. Micro-Computed Tomography Comparison of Preterminal Bronchioles in Centrilobular and Panlobular Emphysema. American journal of respiratory and critical care medicine 2017; 195(5): 630–8. [PubMed: 27611890]

15. Verleden SE, Vasilescu DM, Willems S, et al. The site and nature of airway obstruction after lung transplantation. American journal of respiratory and critical care medicine 2014; 189(3): 292–300. [PubMed: 24354907]

16. Boon M, Verleden SE, Bosch B, et al. Morphometric Analysis of Explant Lungs in Cystic Fibrosis. American journal of respiratory and critical care medicine 2016; 193(5): 516–26. [PubMed: 26551917]

17. Lynch DA, Sverzellati N, Travis WD, et al. Diagnostic criteria for idiopathic pulmonary fibrosis: a Fleischner Society White Paper. Lancet Respir Med 2018; 6(2): 138–53. [PubMed: 29154106]

18. Vasilescu DM, Klinge C, Knudsen L, et al. Stereological assessment of mouse lung parenchyma via nondestructive, multiscale micro-CT imaging validated by light microscopic histology. Journal of applied physiology 2013; 114(6): 716–24. [PubMed: 23264542]

19. Vasilescu DM, Phillion AB, Tanabe N, et al. Nondestructive cryomicro-CT imaging enables structural and molecular analysis of human lung tissue. Journal of applied physiology 2017; 122(1): 161–9. [PubMed: 27856720]

20. Ashcroft T, Simpson JM, Timbrell V. Simple method of estimating severity of pulmonary fibrosis on a numerical scale. J Clin Pathol 1988; 41(4): 467–70. [PubMed: 3366935]

21. Verleden SE, Vasilescu DM, McDonough JE, et al. Linking clinical phenotypes of chronic lung allograft dysfunction to changes in lung structure. Eur Respir J 2015; 46(5): 1430–9. [PubMed: 26113688]

22. Hamman L, Rich AR. Acute Diffuse Interstitial Fibrosis of the Lungs. Bull Johns Hopkins Hospital 1944; 74(March): 177–212.

23. Anderson AE Jr., Foraker AG. Morphological aspects of interstitial pulmonary fibrosis. Arch Pathol 1960; 70: 79–93. [PubMed: 13793353]

24. Coxson HO, Hogg JC, Mayo JR, et al. Quantification of idiopathic pulmonary fibrosis using computed tomography and histology. American journal of respiratory and critical care medicine 1997; 155(5): 1649–56. [PubMed: 9154871]
25. Whitwell F. A study of the pathology and pathogenesis of bronchiectasis. Thorax 1952; 7(3): 213–39. [PubMed: 12984409]
26. Nagaishi C, Nagasawa N. Functional Anatomy and Histology of the Lung: University Park Press; 1972.
27. Hogg JC, Chu F, Utokaparch S, et al. The nature of small-airway obstruction in chronic obstructive pulmonary disease. N Engl J Med 2004; 350(26): 2645–53. [PubMed: 15215480]
28. Abbas AK, Lichtman AH, Pillai S, Baker DL, Baker A. Cellular and molecular immunology. Ninth edition. ed. Philadelphia, PA: Elsevier; 2018.
29. De Sadeleer LJ, Meert C, Yserbyt J, et al. Diagnostic Ability of a Dynamic Multidisciplinary Discussion in Interstitial Lung Diseases: A Retrospective Observational Study of 938 Cases. Chest 2018; 153(6): 1416–23. [PubMed: 29608882]
30. Fischer A, Antoniou KM, Brown KK, et al. An official European Respiratory Society/American Thoracic Society research statement: interstitial pneumonia with autoimmune features. Eur Respir J 2015; 46(4): 976–87. [PubMed: 26160873]
31. Mead J. The lung's "quiet zone". N Engl J Med 1970; 282(23): 1318–9. [PubMed: 5442364]
32. Koo HK, Vasilescu DM, Booth S, et al. Small airways disease in mild and moderate chronic obstructive pulmonary disease: a cross-sectional study. Lancet Respir Med 2018; 6(8): 591–602. [PubMed: 30072106]
33. Kawabata Y, Hoshi E, Murai K, et al. Smoking-related changes in the background lung of specimens resected for lung cancer: a semiquantitative study with correlation to postoperative course. Histopathology 2008; 53(6): 707–14. [PubMed: 19102010]
34. Katzenstein AL, Mukhopadhyay S, Zanardi C, Dexter E. Clinically occult interstitial fibrosis in smokers: classification and significance of a surprisingly common finding in lobectomy specimens. Hum Pathol 2010; 41(3): 316–25. [PubMed: 20004953]
35. Putman RK, Hatabu H, Araki T, et al. Association Between Interstitial Lung Abnormalities and All-Cause Mortality. JAMA 2016; 315(7): 672–81. [PubMed: 26881370]
36. Cottin V, Nunes H, Brillet PY, et al. Combined pulmonary fibrosis and emphysema: a distinct underrecognised entity. Eur Respir J 2005; 26(4): 586–93. [PubMed: 16204587]
37. Galban CJ, Han MK, Boes JL, et al. Computed tomography-based biomarker provides unique signature for diagnosis of COPD phenotypes and disease progression. Nat Med 2012; 18(11): 1711–5. [PubMed: 23042237]
38. Vasilescu DM, Martinez FJ, Marchetti N, et al. Non-Invasive Imaging Biomarker Identifies Small Airway Damage in Severe COPD. American journal of respiratory and critical care medicine 2019.

RESEARCH IN CONTEXT

Evidence before this study

The concept that IPF is an interstitial lung disease that obliterates alveoli but spares the airways is widely accepted in the literature based on the observation that persons affected by IPF can achieve much larger than normal airflows at the low lung volumes where they are forced to breath. At the beginning of this study in January 2017 and prior to submission May 2019, we searched the scientific literature in PubMed (with no date or language restrictions) for the following search terms “Small airways” and “Idiopathic Pulmonary Fibrosis”. We found no publications using combined MDCT, microCT and histology to investigate small airways disease in IPF.

Added value of this study

To the best of our knowledge this report provides direct evidence that in IPF affected lungs the small airways <2mm in diameter increase their visibility due to thickening of their airway walls and distortion of their airway lumens. Further, compared to normal (control) lung anatomy, minimal fibrosis in IPF is also associated with a 60% reduction in the number of terminal bronchioles/ml of lung, as well as the appearance of fibroblastic foci and infiltration of the tissue by inflammatory immune cells capable of forming non-encapsulated lymphoid follicles. Importantly, established fibrosis in IPF did not show a further decline of the terminal bronchioles, but was associated with an increase in airspace size, Ashcroft fibrosis score, volume fraction of tissue and collagen; consistent with progressive fibrosis. These data indicate that the pathology in the small airways is an important feature of IPF.

Implications of all the available evidence

Although these results must be considered preliminary, based on the relatively small number of cases studied to date, they show that compared to normal (control) lung anatomy there is a reduction in the number of terminal bronchioles, the appearance of fibroblastic foci, and lymphoid follicle formation in IPF tissue with minimal fibrosis. In contrast, established fibrosis in IPF tissue is dominated by a progressive fibrotic process that leads to scar formation. Based on these findings, further work is required to understand the role of the small conducting airways in IPF and the potential to therapeutically target them.

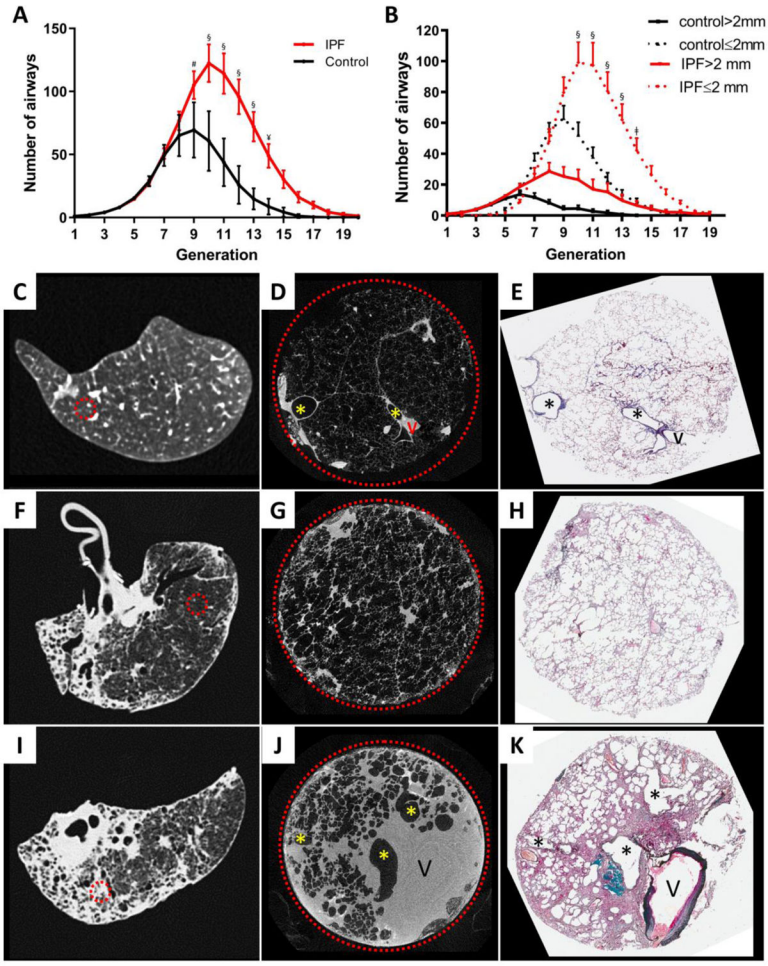

Figure 1:

(A) Comparison of the distribution of mean ± SEM number of airways visible on the airway tree, reconstructed at the 800μM spatial resolution of the MDCT specimen scans at each branching generation shows an increase in the number of visible airway in IPF compared to the control lungs beyond generation 8 in experiment 1. (B). Shows this increase in number occurs primarily in airways ≤2 mm per generation show the greatest increase in visible airways occurs in the airways ≤2 mm in diameter. (C) MDCT specimen scan images of control lung (D and E) lungs affected by IPF where the circled areas represent regions of minimal (D) and established (E) fibrosis, selected by the radiologists who examined the preoperative MDCT scans. MicroCT scans of tissues taken from the circled areas were used for comparisons among control, minimal and established fibrotic regions (F, G, and H, respectively). § = <0·0001, ¥ = 0·0001, # = 0·0023, ǂ = 0·0027, V indicates vessels and * indicates airways.

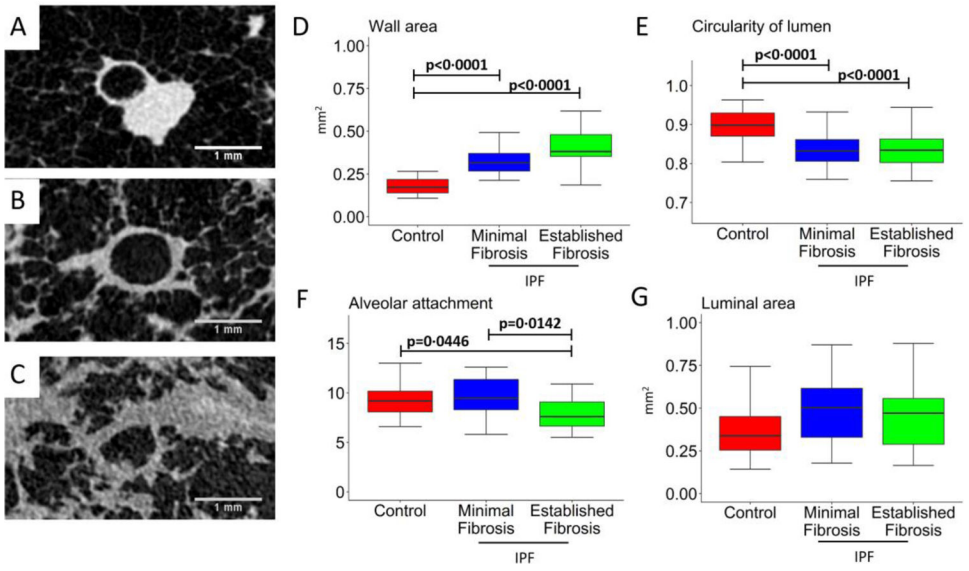

Figure 2:

Representative cross-sectional microCT images of pre-terminal small airways cut at 90 degrees to the centreline (A-C) where the analysis showed an increase in wall area (D) and a reduction in the circularity of the lumen (E) in minimal and established fibrosis. The numbers of alveolar attachments tethered to the outer walls of pre-terminal bronchioles was significantly decreased in established fibrosis (F), and a trend toward a decline in lumen area that did not reach statistical significance (G) in minimal and established fibrosis compared to controls in experiment 2.

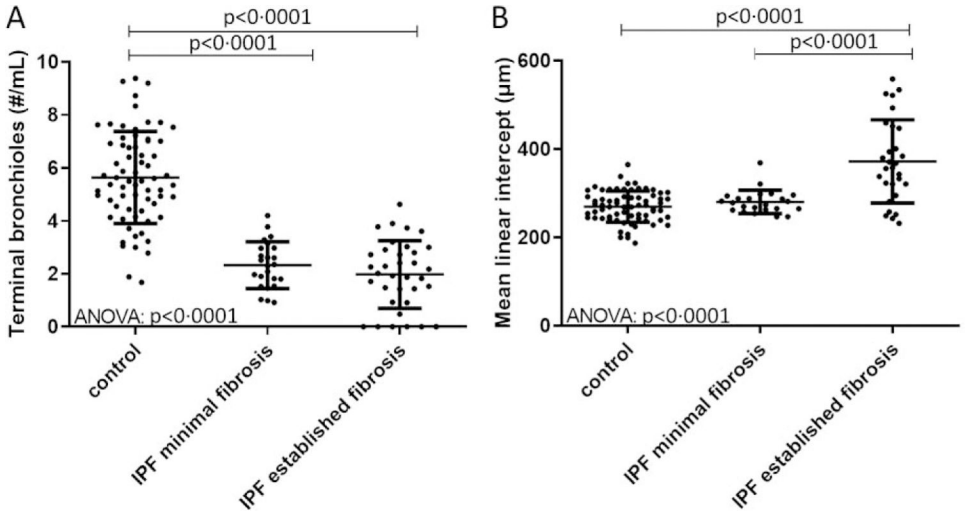

Figure 3:

Shows the number of terminal bronchioles and the mean linear intercept (Lm) in experiment 1. (A) Terminal bronchioles are sharply reduced in number per mL of tissue compared to controls in regions of minimal fibrosis, without further decline between regions of minimal and established fibrosis in IPF. (B) Lm increased in regions of established fibrosis in IPF due to the collapse of alveoli on alveolar ducts Values are expressed as per sample.

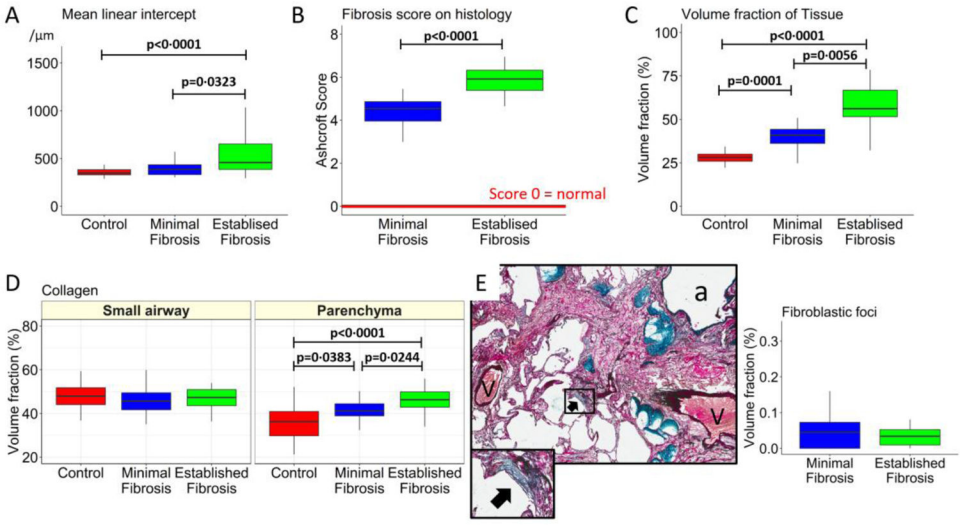

Figure 4:

The progression from control lung anatomy to minimal and established fibrosis is associated with an increase in Lm in experiment 2 (A). (B) The histology-based Ashcroft fibrosis score that ranges between 0 (normal) and 8 (dense fibrosis) was greater in established fibrosis than minimal fibrosis. (C) The volume fraction of the lung samples taken up by tissue. (D) The volume fraction of lung tissue taken up by collagen identified by picro sirius red staining used to identify collagen, in the parenchyma but not the airways. (E) Example of a fibroblastic focus, showing that the volume fraction was similarly increased in both minimal and established fibrosis. Values are expressed as per sample.

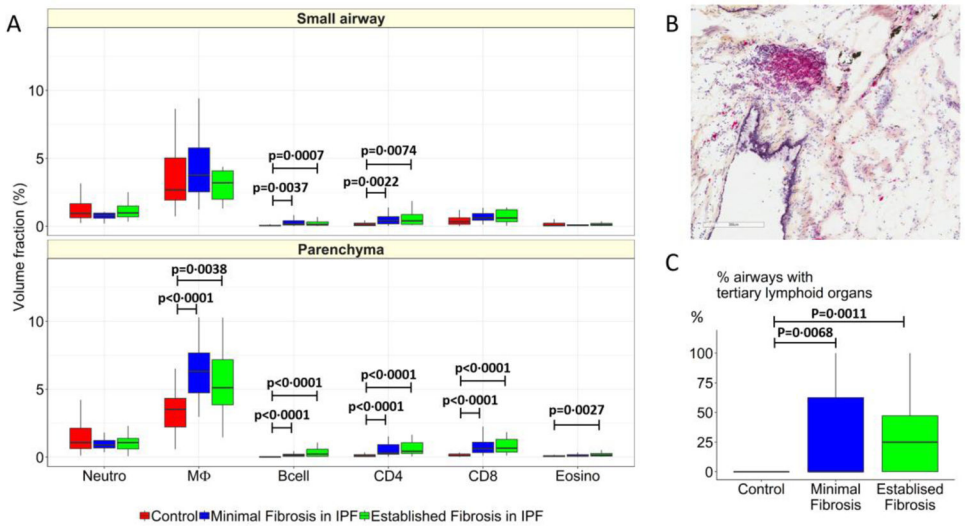

Figure 5:

Compares the volume fractions of infiltrating inflammatory immune cells in control lung tissue (red) to the volume fractions of the same cells in regions of minimal (blue) and established (green) fibrosis in experiment 2. This comparison shows (A) B-cell and CD4 lymphocyte infiltration increased in airways tissue and that the infiltration of macrophages, B-cells, CD4, CD8 and eosinophils are increased in the parenchyma in regions of minimal and established fibrosis compared to controls. These data show that the number airways containing tertiary lymphoid organs, as illustrated in (B), increased in both minimal and established regions of fibrosis compared to controls (C), but were not different from each other in the airways. Values are expressed as per sample.

Table 1:

Patient characteristics in experiments 1 and 2.

	Experiment 1 Random sampling		Experiment 2 Targeted sampling	
	Control	**IPF**	**Control**	**IPF**
Patient Characteristics				
N[†]	8	9	6	9
Sex ratio M/F	7/1	9/0	4/2	9/0
Age	54·0 ± 12·4	57·4 ± 4·8	57·8 ± 4·4	57·2 ± 5·4
Height (cm)	176 ± 6	171 ± 8	176 ± 2	173 ±7
Weight (kg)	81 ± 15	71 ± 11	83 ± 5	72 ± 10
Smoking history (ex/none)	3/5	8/1	2/4	9/0
Pack Years	9 ± 14	16 ± 12	NA	24 ±12
Pulmonary Function				
FEV_1 (% pred)	-	59·2 ± 14·1	-	63·0 ± 16·8
FVC (% pred)	-	54·2 ± 14·0	-	58·9 ± 17·2
TLC (% pred)	-	52·4 ± 11·7	-	56·9 ± 16·6
DLco (% pred)	-	26·6 ± 10·24	-	27·3 ± 8·2
FEV_1/FVC	-	0·88 ± 0·05	-	0·85 ± 0·06
Pre-operative CT				
Airway dilatation (%)	-	55 ± 30	-	50 ± 11
Consolidation (%)	-	2 ± 4	-	2 ± 1
Ground glass opacities (%)	-	46 ± 27	-	57 ± 9
Air trapping (%)	-	9 ± 4	-	8 ± 2
Reticular pattern (%)	-	63 ± 12	-	63 ± 4
Volume loss (%)	-	44 ± 18	-	40 ± 8
Cyst formation (%)	-	49 ± 19	-	53 ± 6
Emphysema (%)	-	7 ± 12	-	19 ± 7

Values given are the means ± standard deviation (SD). FEV_1 denotes forced expiratory volume in 1 second, FVC forced vital capacity post-bronchodilator, and TLC total lung capacity. DLCO/VA denotes the diffusing capacity of the lung for carbon monoxide adjusted for alveolar volume. The severity of disease was graded on the pre-operative CT using the current guidelines.

[†]Seven out of nine patients with IPF and three out of six control subjects in experiment 2 were also included in experiments 1.

Table 2:

Specimen MDCT and microCT analysis in experiments 1 and 2

	Experiment 1 Random sampling			Experiment 2 Targeted sampling		
	Control (N=8)	**IPF (N=9)**	**p value**	**Control (N = 6†)**	**IPF (N = 9†)**	**p value**
Lung specimen CT						
Total Lung volume (L)	3·29 ± 0·61	1·52 ± 0·39	<0·0001	3·35± 0·44	1·60 ± 0·38	0·0004
Lung tissue volume (L)	0·403 ± 0·051	0·598 ± 0·106	0·001	0·369 ± 0·64	0·566 ± 0·140	0·0076
Lung mass (g)	434 ± 53	606 ± 117	0·001	392 ± 68	641 ± 125	0·0016
Lung density (g/L)	134 ± 16	407 ± 59	<0·0001	118 ± 19	409 ± 21	0·0004
No. airways/L of lung	125±36	572±222	<0·0001	NA	NA	NA
Total no. of airways /lung	402±114	811±251	0·0055	NA	NA	NA
Micro CT						
No. sample cores	72	78		36	54	
No. terminal bronchioles /lung	17,914 ± 6,243	3,404 ± 748	<0·0001	13,981 ± 4,029	2,368 ± 1,063	<0·001
No. terminal bronchioles /mL	5·8 ± 0·7	2·3 ± 0·4	<0·0001	4·1 ± 1·5	1·7 ± 1·2	< 0·0001
Minimal Diameter (μm)	370 ± 39	463 ± 59	0·0025	610 ± 149	671 ± 152	0·0480
Minimal area(mm^2) Parenchyma	0·16 ± 0·02	0·25 ± 0·05	0·0002	0·30 ± 0·15	0·37 ± 0·16	0·0480
Lm (μm)	269 ±26	345 ± 54	0·0010	359 ± 53	523 ± 308	0·0001
% of Tissue	23·6 ± 1·7	38·3 ± 5·9	<0·0001	28·4 ± 3·7	48·5 ± 13·3	< 0·0001

Values given are the means ± standard deviation (SD). Values derived from the specimen MDCT scan and No. terminal bronchioles /lung are expressed per case, whereas other values derived from the micro CT scans are expressed per sample. Lm denotes mean linear intercept.

†Seven patients with IPF and 3 control subjects were included in both experiments 1 and 2.